



Improved Therapeutic Window in *BRCA*-mutant Tumors with Antibody-linked Pyrrolobenzodiazepine Dimers with and without PARP Inhibition

Haihong Zhong¹, Cui Chen¹, Ravinder Tammali¹, Shannon Breen¹, Jing Zhang¹, Christine Fazenbaker¹, Maureen Kennedy¹, James Conway¹, Brandon W. Higgs¹, Nicholas Holoweckyj¹, Rajiv Raja¹, Jay Harper¹, Andrew J. Pierce², Ronald Herbst¹, and David A. Tice¹

Abstract

Pyrrolobenzodiazepine dimers (PBD) form cross-links within the minor groove of DNA causing double-strand breaks (DSB). DNA repair genes such as *BRCA1* and *BRCA2* play important roles in homologous recombination repair of DSB. We hypothesized that PBD-based antibody–drug conjugates (ADC) will have enhanced killing of cells in which homologous recombination processes are defective by inactivation of *BRCA1* or *BRCA2* genes. To support this hypothesis, we found 5T4–PBD, a PBD-dimer conjugated to anti-5T4 antibody, elicited more potent antitumor activity in tumor xenografts that carry defects in DNA repair due to *BRCA* mutations compared with *BRCA* wild-type xenografts. To delineate the role of *BRCA1/2* mutations in determining sensitivity to PBD, we used siRNA knockdown and isogenic *BRCA1/2* knockout models to demonstrate that *BRCA* defi-

ciency markedly increased cell sensitivity to PBD-based ADCs. To understand the translational potential of treating patients with *BRCA* deficiency using PBD-based ADCs, we conducted a "mouse clinical trial" on 23 patient-derived xenograft (PDX) models bearing mutations in *BRCA1* or *BRCA2*. Of these PDX models, 61% to 74% had tumor stasis or regression when treated with a single dose of 0.3 mg/kg or three fractionated doses of 0.1 mg/kg of a PBD-based ADC. Furthermore, a suboptimal dose of PBD-based ADC in combination with olaparib resulted in significantly improved antitumor effects, was not associated with myelotoxicity, and was well tolerated. In conclusion, PBD-based ADC alone or in combination with a PARP inhibitor may have improved therapeutic window in patients with cancer carrying *BRCA* mutations.

Introduction

Antibody–drug conjugates (ADC) are an emerging novel class of anticancer treatment agents that provide improved target specificity and potency. Four ADCs have been approved so far, ado-trastuzumab emtansine, brentuximab vedotin, inotuzumab ozogamicin, and gemtuzumab ozogamicin. However, most ADCs still fail due to dose-limiting toxicities on critical normal tissues occurring at doses too low to achieve antitumor activity (1). Therefore, one of the major challenges to ADCs is the narrow therapeutic index. In recent years, significant advances in engineering new linker and conjugation technologies together with novel highly cytotoxic payload have been made in an effort to

develop safer, more effective ADCs. Most cytotoxic payloads used in ADCs currently under investigation are microtubule inhibitors and DNA-damaging drugs. The tubulin inhibitors, such as auristatin and maytansinoid, are potent cytotoxic agents against cultured cancer cells, with IC₅₀ values in the picomolar range as free drugs (2, 3). The DNA-damaging agents, such as duocarmycin and calicheamicin are powerful antitumor antibiotics that bind to the minor groove of DNA. Another new category of DNA-damaging agent is pyrrolobenzodiazepine dimers (PBD). PBD dimers bind in the minor groove of DNA and crosslink opposite strands causing double-strand breaks (DSB; ref. 4). It has been shown that PBD dimers have very potent cytotoxicity with 10-fold lower IC₅₀ compared with auristatins and maytansinoids with activity against a broad spectrum of tumors (5–8). PBD dimers and PBD-based ADCs are currently being evaluated in clinical trials with more anticipated to enter clinical development over the next few years (9–11).

The repair of DSB is accomplished by two main DNA damage repair mechanisms: homologous recombination (HR) and non-homologous end joining. HR uses a homologous DNA template and can repair DSB with high fidelity. *BRCA1* and *BRCA2* are key mediators involved in repairing DSB via HR (12). When mutated, these genes are associated with familial breast and ovarian cancer. Approximately 10%–20% of breast and ovarian cancers are attributed to germline mutations in *BRCA1/2* genes (13, 14).

¹Oncology Research, MedImmune, Gaithersburg, Maryland. ²Translational Science – Oncology, Innovative Medicines and Early Development, AstraZeneca, Cambridge, United Kingdom.

Note: Supplementary data for this article are available at Molecular Cancer Therapeutics Online (<http://mct.aacrjournals.org/>).

Corresponding Authors: Haihong Zhong, MedImmune, LLC, One MedImmune Way, Gaithersburg, MD 20878. Phone/Fax: 301-398-5343; E-mail: zhongh@medimmune.com; and David A. Tice, Phone/Fax: 301-398-4592; E-mail: ticed@medimmune.com

doi: 10.1158/1535-7163.MCT-18-0314

©2018 American Association for Cancer Research.

Normal tissues are heterozygous and retain a wild-type copy of the *BRCA* gene, while tumors lose the functional allele and become homozygous for *BRCA* deficiency. *BRCA*-mutated cells exhibit enhanced sensitivity to DNA interstrand cross-linking agents including platinum-based chemotherapeutic drugs, melphalan, topoisomerase II inhibitors, and inhibitors of PARP (15, 16). PARP is a DNA-binding protein that binds and removes the damaged region of DNA (17). PARP inhibitors (PARPi) have been shown to induce synthetic lethality in *BRCA*-mutated cancer cells (18, 19). In the clinic, PARPi, such as olaparib and rucaparib, significantly improved progression-free survival in patients with germline *BRCA* mutations as single agent, and have gained FDA approval (20–22). Other PARPi, including veliparib, talazoparib, and niraparib, are currently being accessed in clinical trials and showing promising results (23–25). Despite the profound and sustained antitumor response in patients harboring *BRCA* mutations, PARPi has not yet demonstrated significant improvement in overall survival (26–28). PARPi combination therapy has been evaluated extensively over the last decade. A number of preclinical studies have shown that PARP inhibition can enhance the effects of agents that induce DNA damage such as ionizing radiation and some chemotherapeutics in cancer types such as breast, ovarian, lung, melanoma, and prostate cancers (29–33). This includes the first combination of a PARPi with an ADC, IMMU-132, which employs a topoisomerase I inhibitor (34).

We hypothesized that because PBD dimers cause DNA damage by cross-linking, PBD-based ADCs will have enhanced killing of cells in which HR processes are defective by inactivation of *BRCA1* or *BRCA2* genes. In this article, we provide evidence that knocking down or mutating *BRCA1* or *BRCA2* genes by genetic approaches sensitized cells to PBD and a PBD-based ADC. In addition, enhanced efficacy was observed upon combining olaparib with a less than full monotherapy dose of PBD-based ADC in *BRCA2*-deleted xenograft models. Furthermore, combination therapy was not associated with myelotoxicity and was well tolerated in mice, indicating an improved therapeutic window. The marked sensitivity of *BRCA*-deficient tumors to PBD-based ADC alone and its combination with PARPi may have important implications for optimal treatment of patients with breast and ovarian cancer carrying *BRCA* mutations.

Materials and Methods

Cells and reagents

Breast cancer cell lines MDA-MB-361, SUM149PT, and MDA-MB-436, pancreatic cancer cell line Capan-1, and HeLa cells were purchased from ATCC. DLD-1, DLD-1 *BRCA2*^{-/-}, MCF10A, and MCF10A *BRCA1*(185delAG/+) cells were purchased from Horizon Discovery Ltd. Upon delivery, cells were expanded and low passage vials were stored in liquid nitrogen. Studies were carried out within 8 weeks after resuscitation. Cell line authentication was conducted using short tandem repeat–based DNA fingerprinting and multiplex PCR. IMPACT tests were also performed on all cell lines. CellTiter-Glo (CTG) Reagents were obtained from Promega. For *in vitro* studies, olaparib (LC Laboratories) was dissolved in DMSO and diluted by culture media before use. ELISA kits for γ H2AX were purchased from R&D Systems.

γ H2AX immunofluorescence and ELISA assay

γ H2AX immunofluorescence (IF) staining was done using a chamber slide staining assay. DLD-1 and DLD-1 *BRCA2*^{-/-} were

plated 2.5×10^4 cells/well in 8-well, collagen-coated chamber slides in 10% FBS DMEM. On the next day, medium containing 1 μ g/mL cisplatin or 10 ng/mL 5T4–PBD or 100 ng/mL 5T4–PBD were added to the treatment wells. After 24 hours, cells were fixed and permeabilized. Cells were then incubated with primary antibody (phospho-histone H2A.X, Cell Signaling Technology) at room temperature for 1 hour, followed by incubation with secondary antibody [goat anti-rabbit IgG (H+L) Alexa Fluor 647 conjugate, Thermo Fisher Scientific] for 1 hour, and mounted using DAPI-containing mounting media. Images were captured using a confocal microscope.

γ H2AX Pharmacodynamic Assay Kit was purchased from Trevigen, Inc. Assay was performed following the manufacturer's protocol.

siRNA knockdown experiment

HeLa cells were transfected with siRNA directed against *BRCA1* or *BRCA2* genes (ON- TARGETplus SMARTpool reagents, Dharmacon) and a negative control *GAPDH* gene (ON- TARGETplus siCONTROL Non-targeting Pool reagent, Dharmacon) using RNAiMax Transfection Reagent (Life Technologies) for 48 hours according to manufacturer's instructions. After that, cells were treated with either PBD (SG3199) or 5T4–PBD in the medium containing 10% FBS for 5 days. Cell viability was measured by CTG Reagent (Promega).

qRT-PCR analysis

HeLa cells were transfected using siRNA directed against *BRCA1*, *BRCA2*, and *GAPDH* genes as described above. After 48 hours, cells were lysed using Cells to Ct Kit (Ambion) and qRT-PCR analysis was performed with EXPRESS One-Step Superscript qRT-PCR Kit using probes against *BRCA1*, *BRCA2*, and *GAPDH*. 18S rRNA was used as a housekeeping gene for normalization of samples (Thermo Fisher Scientific).

BRCA mutation characterization in patient-derived xenograft tumors

Whole-exome sequencing (WES) was performed on 23 patient-derived xenograft (PDX) samples. DNA was isolated using QIAamp DNA Mini Kit (Qiagen) and 3 μ g were randomly fragmented to an average peak size of 200 bp using Covaris M220 (Covaris). Agilent Sure Select Human All Exon V6 baits were utilized for exome capture and the WES library preparation was performed following the manufacturer's protocol (Agilent SureSelect^{XT} Target Enrichment System for Illumina Multiplexed Sequencing). The quality and quantity of the libraries were evaluated using an Agilent Bioanalyzer 2200 (Agilent) in conjunction with KAPA Library Quantification Kit (Kapa Biosystems). The WES libraries were sequenced on an Illumina NextSeq 500 instrument at 2×100 bp using NextSeq 500/550 v2 Reagent Kits (Illumina).

Sequencing reads were aligned to the human hg19 reference genome (UCSC hg19; Feb 2009 release; Genome Reference Consortium GRCh37) using Bowtie 2 (35). Duplicate reads were identified and removed using Picard. Samtools was applied to bam files from all PDX models to create a single summary of coverage for mapped reads. Bcftools was used to call variants and generate a single VCF file for all PDX models. Functional annotation was assigned to variants with ANNOVAR, which assigned annotation from selected databases (RefGene, 1000 Genome Project, Phast Cons, Genomic Super Dups, ESP6500, LBJ, and

COSMIC). Variants were filtered to include only nonsynonymous, stop gain or loss, or frameshift insertion or deletion. Variants were further filtered to include only rare occurrences by retaining variants with $MAF \leq 0.05$, or no presence in the 1000 Genome Project database.

Raw sequencing data has been deposited in SRA database. The accession number is PRJNA494524.

Xenograft studies in mice

All procedures using mice were approved by the MedImmune Institutional Animal Care and Use Committee according to established guidelines. For *in vivo* efficacy studies, 5×10^6 or 1×10^7 cells in 50% Matrigel were inoculated subcutaneously into female athymic nude mice (Harlan Laboratories). When tumors reached approximately 150–200 mm³, mice were randomly assigned into groups (8–10 mice per group). 5T4-PBD was administered intravenously as a single dose at indicated doses. Olaparib was solubilized in DMSO and diluted in water containing 15% Hydroxypropyl betadex (Sigma) before administering by oral gavage daily at indicated dose. Tumor volumes were measured twice weekly with calipers. Tumor growth inhibition was calculated using the formula $\frac{1}{2} \times L \times W^2$ (L , length; W , width). Body weights were measured twice weekly to assess tolerability of the treatments. Two-way ANOVA was used to compare the reduction in tumor volume in mice treated with the combination therapies versus those treated with either agent alone.

For hematologic toxicity study, athymic *nu/nu* nude mice received either olaparib (100 mg/kg, oral gavage, day 0–15), or 5T4-PBD (0.1 mg/kg, intravenous, single dose on day 0), or the combination of both. Whole blood (50 μ L) was drawn through orbital bleeding and was transferred to EDTA tubes. Complete blood count was determined using the Sysmex XT-2000 hematology analyzer.

Results

Enhanced killing of *BRCA1*- or *BRCA2*-deficient xenograft tumors compared with *BRCA* wild-type tumors

5T4-PBD (MEDI0641) is an ADC in which anti-5T4 antibody was site-specifically conjugated to two PBD dimers (SG3249) per antibody. It has been shown to elicit a potent antitumor response in 5T4-positive xenograft models (36). In the process of characterizing 5T4-PBD, we noticed that it had superior antitumor activity in the models that carry *BRCA* mutations. To fully understand the efficacy of the PBD-based ADC in *BRCA*-mutated xenograft tumors, we established *BRCA* wild-type and *BRCA*-mutated xenograft models. *BRCA* wild-type xenografts include two breast cancer models that have high 5T4 surface expression (MDA-MB-361, MDA-MB-468) and one lung cancer model NCI-H1975 with low to medium 5T4 expression. *BRCA*-mutated xenograft models include two breast cancer models with *BRCA1* mutation that express high or medium levels of surface 5T4 (SUM149PT and MDA-MB-436), and one pancreatic cancer xenograft model that has low levels of surface 5T4 and is *BRCA2* deficient (Capan-1). Treatment of mice bearing *BRCA* wild-type xenografts with a single dose of 5T4-PBD at 0.3 mg/kg resulted in tumor stasis followed by tumor regrowth (Fig. 1A). However, treatment of mice bearing *BRCA*-mutated xenografts with a single dose of 5T4-PBD at 0.3 mg/kg resulted in tumor regression (Fig. 1B). Even treatment with the low dose of

0.1 mg/kg resulted in tumor regression in two of the *BRCA*-deficient models. Isotype control ADC demonstrated more impact in *BRCA*-mutant models compared with wild-type, again suggesting that the cells are more sensitive to the PBD regardless of whether it enters the cell in a target-specific or nonspecific manner. Overall, the PBD-based ADC was more potent in *BRCA*-deficient xenograft models compared with wild-type xenografts, regardless of target expression levels consistent with a role for *BRCA1/2* in repair of DNA interstrand crosslinks and related downstream DNA damage.

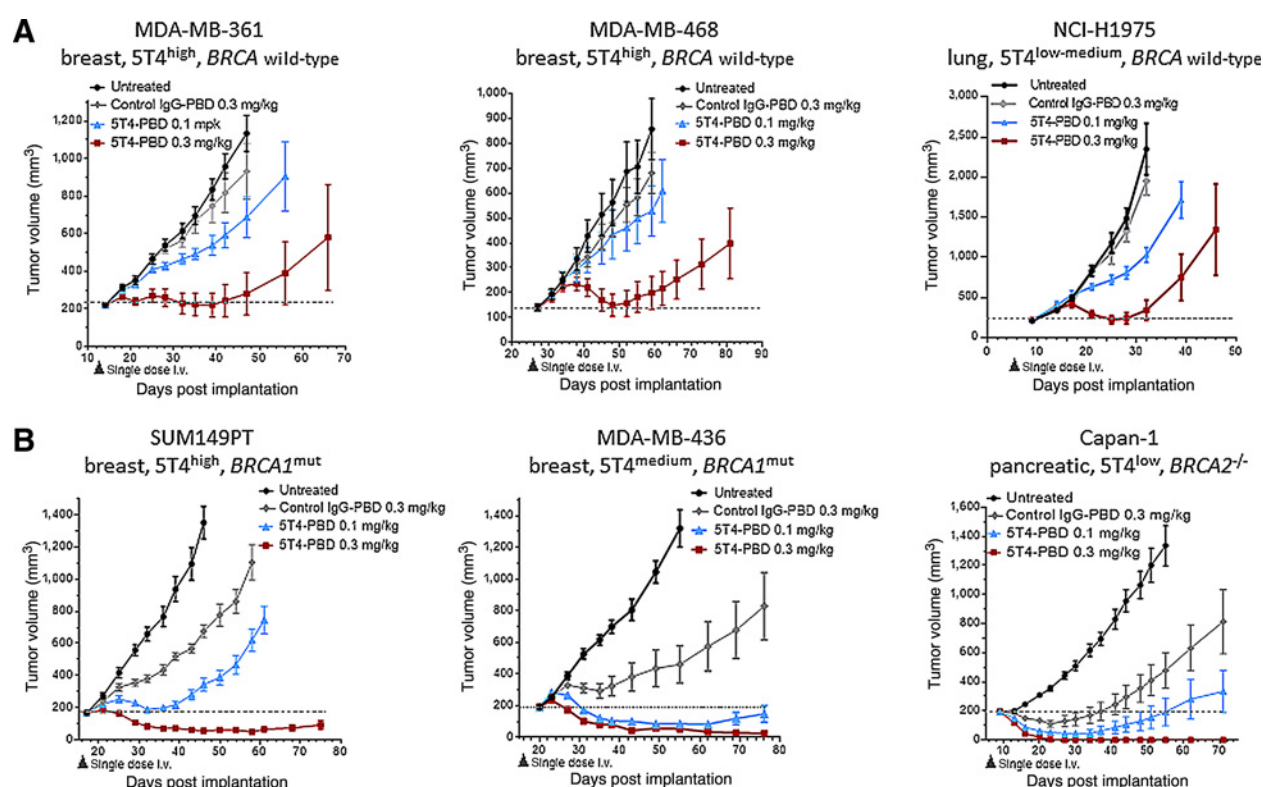
DNA repair defects from genetic deletion of *BRCA1/2* markedly increases antitumor activity of a PBD-based ADC

To investigate *BRCA* as a determinant of sensitivity to PBD, we used siRNA to knockdown *BRCA1* or *BRCA2* genes in DNA repair wild-type HeLa cells. qPCR and Western blot analysis demonstrated nearly complete depletion of *BRCA1* and *BRCA2* at mRNA and protein levels. Suppression of *BRCA1* or *BRCA2* resulted in 5- to 10-fold increase in sensitivity to PBD and 5T4-PBD (Supplementary Fig. S1).

To further demonstrate the role of *BRCA* genes in determining sensitivity to PBD-based ADCs, we used isogenic models of *BRCA1* or *BRCA2* deficiency. MCF10A *BRCA1*(185delAG/+) is a breast epithelial cell line with heterozygous knocking of a 2-bp deletion resulting in a premature stop codon at position 39, terminating *BRCA1* protein expression (37) versus the *BRCA1* wild-type parental MCF10A line. DLD1 *BRCA2*^{-/-} is a colorectal adenocarcinoma cell line with homozygous deletion of exon 11 of the *BRCA2* gene (15), engineered from *BRCA2* wild-type DLD1 cells. The use of isogenic cell pairs allowed us to exclude many other unknown factors that could contribute to the differential sensitivity in nonisogenic systems. FACS analysis demonstrated that both parental and *BRCA*-deficient cells had equivalent 5T4 surface expression (Fig. 2A; Supplementary Fig. S2A). MCF10A *BRCA1*(185delAG/+) and DLD1 *BRCA2*^{-/-} cells were 5-fold and 24-fold more sensitive to 5T4-PBD in cytotoxicity assays compared with their wild-type cells, respectively (Fig. 2B; Supplementary Fig. S2B).

To examine effects of *BRCA* deficiency on antitumor activity *in vivo*, we grew DLD1 parental and DLD1 *BRCA2*^{-/-} xenografts subcutaneously in nude mice and compared tumor growth following administration of a single dose of 5T4-PBD at 0.1, 0.3, and 1 mg/kg. 0.1 mg/kg of 5T4-PBD was inactive against DLD1 wild-type tumor. There was modest tumor growth inhibition of DLD1 tumors observed with 5T4-PBD treatment at 0.3 and 1.0 mg/kg (Fig. 2C, top). In contrast, even though DLD1 *BRCA2*^{-/-} tumors grew slower than DLD1 wild-type parental tumors, a single dose of 5T4-PBD at 0.1 mg/kg significantly inhibited growth of DLD1 *BRCA2*^{-/-} tumor xenografts, with tumor regression seen at 0.3 and 1.0 mg/kg (Fig. 2C, bottom), suggesting *BRCA2* deficiency markedly sensitized DLD1 tumors to the DNA damage caused by the PBD-based ADC.

To examine the extent of DNA damage in response to PBD-based ADC treatment, we evaluated γ H2AX foci formation, a well-established biomarker of DNA damage (38). γ H2AX IF staining was notably stronger in *BRCA2*^{-/-} cells as compared with wild-type cells upon 5T4-PBD treatment (Fig. 2D). We also quantified expression of γ H2AX protein using an ELISA-based γ H2AX pharmacodynamic assay. Expression of γ H2AX was elevated in all treatment groups compared with untreated control in both DLD1 *BRCA2*^{-/-} and wild-type lines; however, the increase associated

**Figure 1.**

In vivo efficacy of 5T4-PBD in *BRCA* wild-type or *BRCA*-deficient cancer xenograft models. A single dose of 5T4-PBD was administered at 0.1 and 0.3 mg/kg intravenously into nude mice bearing *BRCA* wild-type tumors (MDA-MB-361, MDA-MB-468, and NCI-H1975; **A**), or *BRCA*-deficient tumors (SUM149PT, MDA-MB-436, and Capan-1; **B**). 5T4 expression in tumor cell lines was determined by FACS analysis and annotated as 5T4 high, medium, and low.

with 5T4-PBD treatment in *BRCA2*^{-/-} cells was statistically significant (Fig. 2D). Interestingly, increased γ H2AX were readily detected in untreated *BRCA2*^{-/-} cells compared with untreated parental cells consistent with an intrinsic HR defect.

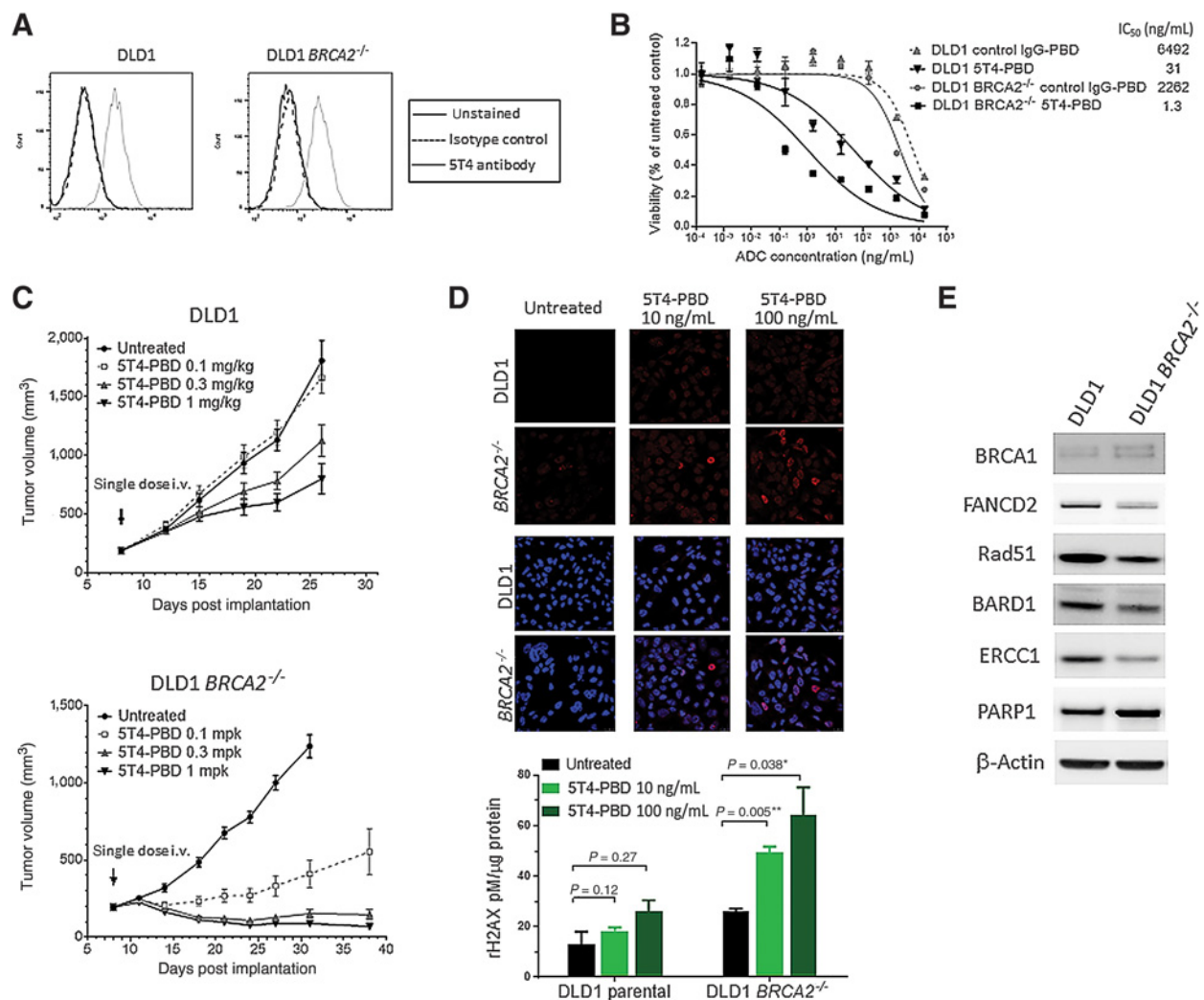
Of interest, we noticed that baseline levels of other HR repair (HRR) proteins such as FANCD2, Rad51, and BARD1, and DNA excision repair protein ERCC1 were higher in DLD1 cells than those in DLD1 *BRCA2*^{-/-} cells (Fig. 2E). It is possible that the high expression of other HRR proteins in DLD1 cells may result in more efficient repair of damaged DNA induced by 5T4-PBD. The decreased expression of HRR proteins in DLD1 *BRCA2*^{-/-} cells may contribute to the greater sensitivity to PBD-based ADC. DLD1 *BRCA2*^{-/-} cells also had increased protein expression of PARP1 compared with parental DLD1 cells.

Pharmacologic response across *BRCA*-deficient PDX models

To understand the translational potential of treating patients with *BRCA* deficiency using PBD-based ADCs, we collected 23 breast and ovarian PDX models that were deficient for either *BRCA1* ($n = 12$) or *BRCA2* ($n = 6$) or both genes ($n = 5$; Supplementary Table S1) and assessed the efficacy of 5T4-PBD. Mice were treated with 5T4-PBD administered as either a single dose of 0.3 mg/kg or as three fractionated doses of 0.1 mg/kg. When administered as single dose at 0.3 mg/kg, 17 PDXs [73.9% DCR (disease control rate)] demonstrated complete regression (CR), partial regression (PR), and stable disease (SD; Supplementary Fig. S3). We then tested the dosing regimen of

0.1 mg/kg given every 3 weeks for a total of 3 doses. DCR rate was 60.8% (14/23 models). In some models, tumor regressions including CRs were already observed after first dose of 0.1 mg/kg (Supplementary Fig. S3). In contrast, neither dosing regimen resulted in a response in 3 *BRCA* wild-type PDX models (Supplementary Fig. S4). The 5T4-PBD was well-tolerated with no body weight loss reported in any of the PDX models.

We performed retrospective analysis of 5T4 expression in untreated PDX tumors using methods described previously (36). IHC analysis demonstrated a wide range of 5T4 staining patterns across 23 *BRCA*-deficient and 3 *BRCA* wild-type PDX models. Each tumor was assessed with membrane staining and given two scores, intensity score (IS; 1+, 2+, and 3+) and frequency score (FS; proportion of positive tumor cells across majority of section where 1 is <10% of tumor cells staining positive, 2 = 11%–24%, 3 = 25%–49%, 4 = 50%–75%, and 5 \geq 75%). The final IHC score of each tumor was calculated using the formula of IS \times FS. The tumors were then divided into 3 groups based on the following criteria: (i) IHC score 1 had IS \times FS score \leq 5; (ii) IHC score 2 was categorized as 5 < IS \times FS \leq 10; and (iii) 10 < IS \times FS \leq 15 was considered as IHC score 3. Representative IHC images are shown in Supplementary Fig. S5. Figure 3 depicts waterfall plots of the antitumor effect of 5T4-PBD dosed at 0.3 and 0.1 mg/kg with an integration of the IHC scores for each PDX model. The data indicated no correlation between 5T4 expression and sensitivity to 5T4-PBD in these *BRCA*-deficient PDX tumors.

**Figure 2.**

Genetic deletion of *BRCA2* augments antitumor activity of PBD-based ADC *in vitro* and *in vivo*. **A**, Flow cytometric analysis of 5T4 surface expression in DLD1 parental and *BRCA2*^{-/-} cells. **B**, Dose-response curves from *in vitro* cell viability assays in DLD1 isogenic cells. Cell viability was calculated by normalizing to untreated cells. **C**, Tumor volumes of DLD1 parental tumors (top) or DLD1 *BRCA2*^{-/-} tumors (bottom) in nude mice administered with single dose of 5T4-PBD intravenously at dose levels of 0.1, 0.3, and 1 mg/kg. **D**, Treatment with 5T4-PBD induces enhanced DNA damage in *BRCA2*^{-/-} cells. IHC staining of γH2AX (red) and DAPI (blue) in DLD1 wild-type or DLD1 *BRCA2*^{-/-} cells treated with ADC dilution buffer or 5T4-PBD (10 or 100 ng/mL) for 24 hours. Graph represents quantitation of γH2AX formation using a γH2AX Pharmacodynamic Assay. *P* values were calculated by Student *t* test. **E**, Western blot analysis of HRR proteins expression in DLD1 and DLD1 *BRCA2*^{-/-} cells.

Combination with olaparib further enhances the antitumor activity of a PBD-based ADC in *BRCA2*^{-/-} tumors

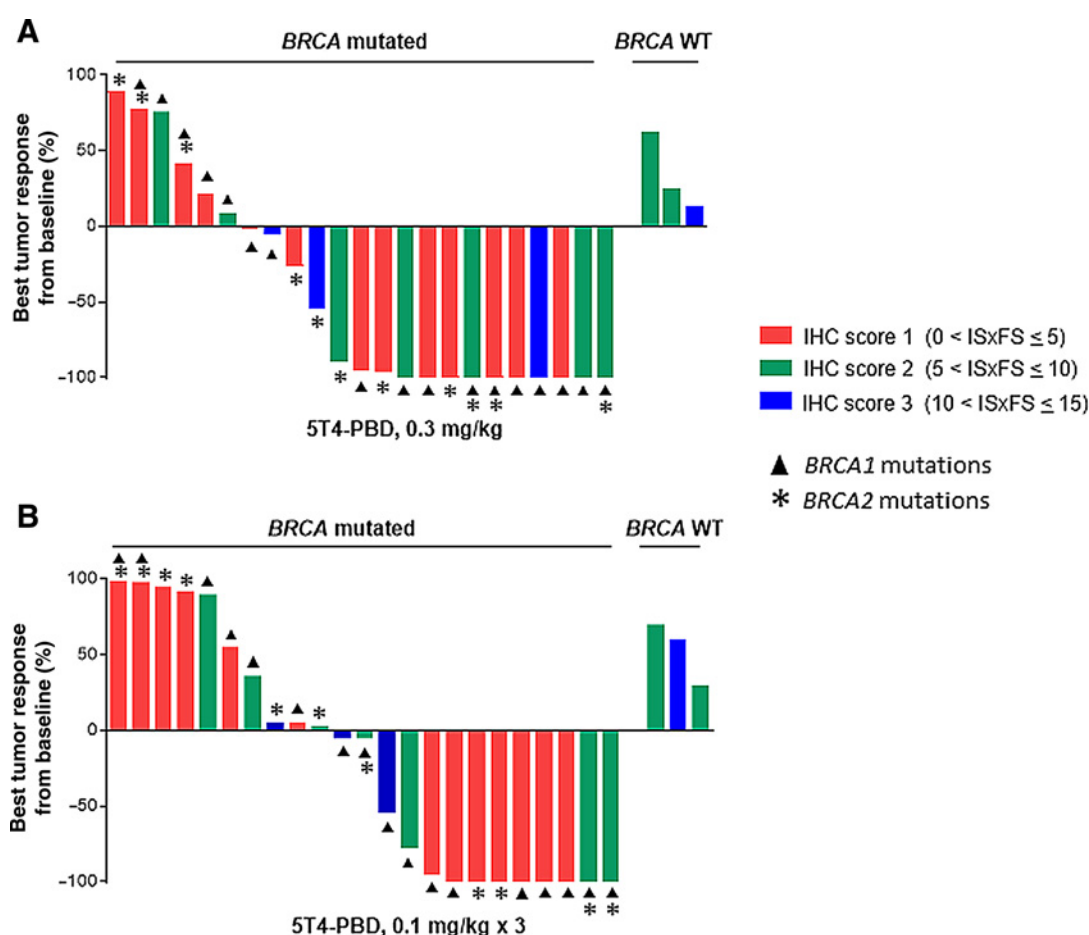
BRCA-deficient cells are known to be more sensitive to PARPi compared with wild-type *BRCA* cells (18, 19). Using DLD1 isogenic cells, we found similar to published results that *BRCA2*^{-/-} cells were as much as over 200-fold more sensitive to olaparib compared with *BRCA* wild-type cells in a cytotoxicity assay (Fig. 4A).

The findings demonstrating an increased sensitivity of *BRCA*-mutated cells to either PBD-based ADCs or olaparib prompted us to consider combination strategies that could potentially lead to an enhanced antitumor effect compared with single-agent therapy. We first used *in vitro* cytotoxicity assays to evaluate the efficacy of suboptimal doses of 5T4-PBD and olaparib alone or in

combination in DLD1 parental and *BRCA2*^{-/-} cells. In DLD1 parental cells, a minimal cytotoxic effect was observed with combination treatment. However, in *BRCA2*^{-/-} cells, when 5T4-PBD was combined with olaparib, a significantly higher percentage of cell death was induced compared with either agent alone (Fig. 4B).

The combination of 5T4-PBD with olaparib was also assessed *in vivo* in the DLD1 and DLD1 *BRCA2*^{-/-} xenograft models. In the DLD1 xenograft model, olaparib had a minimal effect on tumor growth, whereas 5T4-PBD dosed at a high dose of 1 mg/kg showed 66% tumor growth inhibition. However, the combination failed to improve efficacy in this model (Fig. 4C, left). On the other hand, olaparib demonstrated some degree of antitumor activity in the DLD1 *BRCA2*^{-/-} xenograft model (59%

Zhong et al.

**Figure 3.**

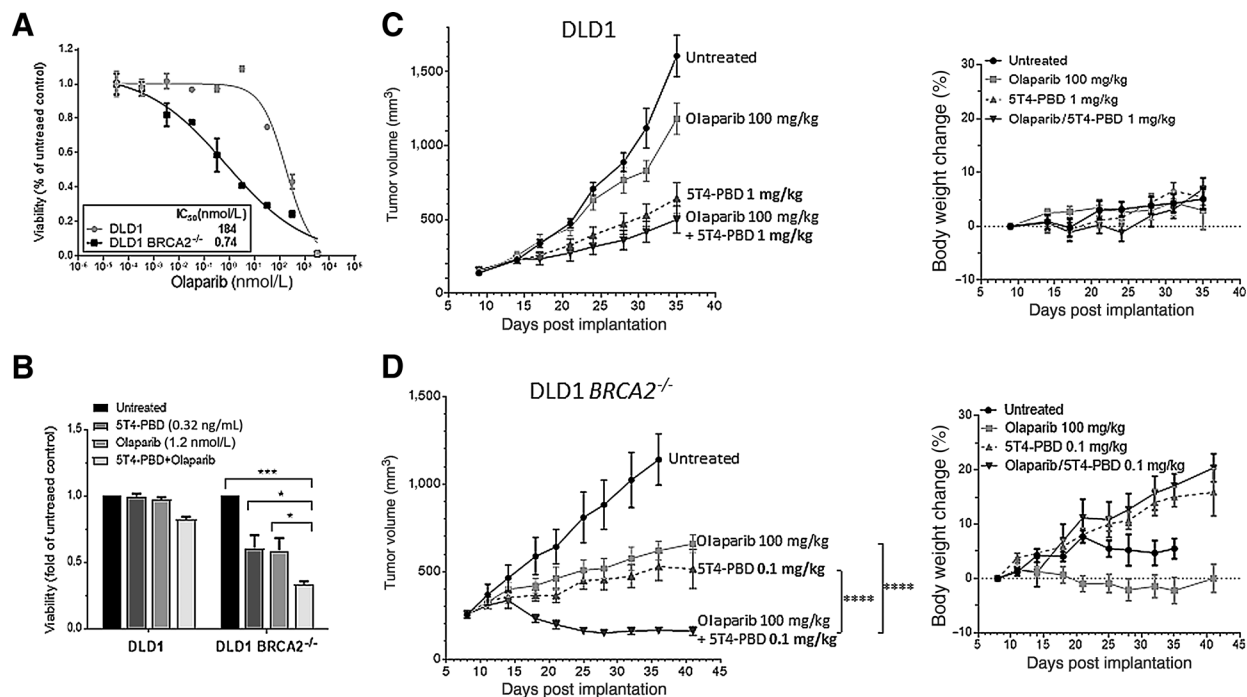
Pharmacologic response to PBD-based ADC across *BRCA*-deficient PDX populations. Breast (18) and ovarian (5) PDX models with *BRCA* mutations or deletions ($n = 2-3$ mice per group) were treated intravenously with 5T4-PBD at 0.3 mg/kg single dose (A), or 0.1 mg/kg every 3 weeks \times 3 dosing regimen (B). Waterfall plots illustrate the best response indicated by percentage tumor volume change from baseline in all PDX tumors on study. Each untreated tumor was stained and scored for 5T4 expression. Colored bars represent individual tumors and colors correspond to the IHC scores. Solid bars are breast PDX models, and patterned bars are ovarian PDX models. Tumor growth curves on individual PDX models can be found in Supplementary Figs. S3 and S4.

TGI; Fig. 4D, left). Consistent with the data in Fig. 2C, 5T4-PBD treatment was efficacious as a single agent at a dose as low as 0.1 mg/kg in DLD1 *BRCA2*^{-/-} tumor (69% TGI). Combining olaparib with 0.1 mg/kg 5T4-PBD resulted in tumor regression (111% TGI), a significantly improved efficacy compared with either single-agent alone (Fig. 4D, left). We also noticed that animals in the 5T4-PBD or combination treatment groups showed body weight gain compared with those treated with olaparib alone. This trend was much more obvious in mice bearing DLD1 *BRCA2*^{-/-} tumor, suggesting a benefit of the combination in tolerability/safety in addition to efficacy (Fig. 4D, right), perhaps in part due to significantly reduced tumor burden.

Combination of PBD-based ADC and olaparib is not associated with any increased hematologic toxicity compared with single-agent alone

Olaparib toxicities in human include thrombocytopenia and grade 3 fatigue (39). In preclinical toxicity studies, the primary target organ of olaparib was bone marrow, with associated changes in peripheral hematology parameters. Currently, only

a limited number of PBD-based ADCs are in clinical trials. Initial toxicities that have been reported include neutropenia, low platelet counts, and skin rash (10, 11). We decided to look at the hematologic profile of combining olaparib with 5T4-PBD to see whether the combination would be associated with any increased toxicities. We did the study in naïve mice to examine the possible off-target toxicities as 5T4 antibody does not cross react with the mouse 5T4 antigen. The doses and dosing schedule were the same as used in the DLD1 *BRCA2*^{-/-} efficacy study at which optimal antitumor activity was observed (Fig. 4D). On day 0, mice were administered a single dose of 5T4-PBD at 0.1 mg/kg and daily olaparib therapy (100 mg/kg) up to day 15. Blood samples were collected at indicated time points and complete blood counts were measured. Despite some significant decreases in white blood cells, monocyte, and lymphocyte upon olaparib treatment on day 9, the counts all recovered once olaparib dosing was stopped (day 20, day 27; Fig. 5). Mice treated with 5T4-PBD monotherapy did not demonstrate changes in any parameters up to day 27 (Fig. 5). Importantly, olaparib plus 5T4-PBD treatment was well tolerated. The only significant drop was found in monocyte counts on

**Figure 4.**

Effect of 5T4-PBD in combination with olaparib. **A**, *In vitro* cell viability assay of olaparib in DLD1 and DLD1 *BRCA2*^{-/-} isogenic cells. **B**, *In vitro* cell viability assay testing the combination of 5T4-PBD with olaparib in DLD1 and DLD1 *BRCA2*^{-/-} isogenic cells. Statistical significance was assessed using Student *t* test (***, *P* < 0.001; *, *P* < 0.05). **C**, Combination of 5T4-PBD with olaparib in DLD1 xenograft model. 5T4-PBD (1 mg/kg) was given as single dose intravenously on day 9 post tumor implantation. Olaparib (100 mg/kg) was dosed daily by oral gavage starting on day 9 ending on day 34. **D**, Combination of 5T4-PBD with olaparib in DLD1 *BRCA2*^{-/-} xenograft model. 5T4-PBD was dosed at 0.1 mg/kg on day 8. Olaparib was dosed daily by oral gavage starting on day 8 ending on day 35. Statistical significance was evaluated using two-way ANOVA (****, *P* < 0.0001).

day 9, which mirrored the olaparib single agent showing full recovery after olaparib dosing was stopped (day 20, day 27; Fig. 5). Together, the results indicate that the combination of olaparib with low dose level of 5T4-PBD improves efficacy as demonstrated in Fig. 4D, and does not cause significant myelotoxicity. It further suggests a wider therapeutic window for the combination strategy in treating *BRCA*-mutated tumors.

Discussion

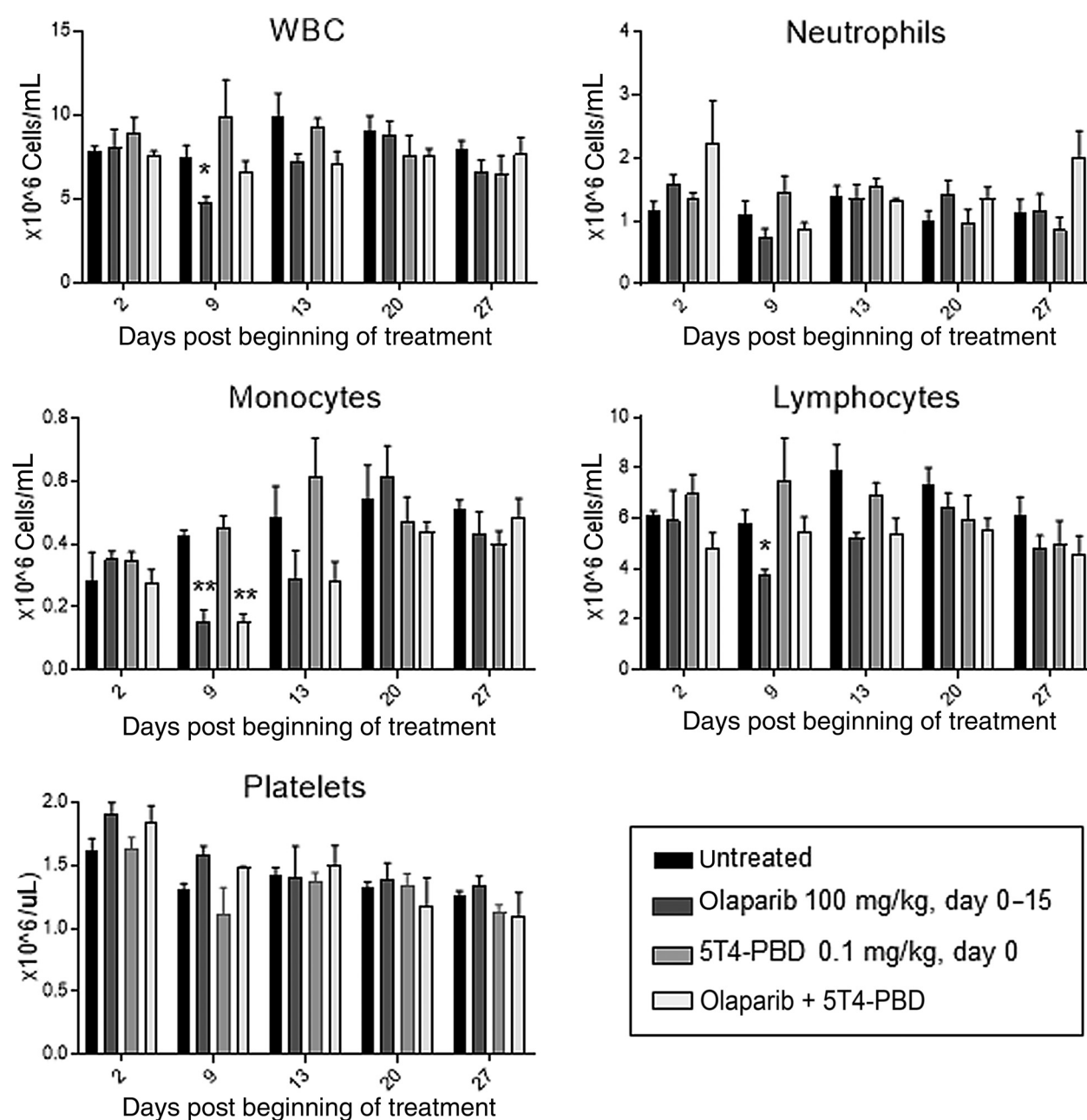
The concept of an ADC is to direct the action of the chemotherapeutic drug to maximize the impact in tumor while minimizing the damage to normal tissues. While some clinical success and validation of this technology has been realized, the vast majority of ADCs have failed in the clinic due to lack of therapeutic index. These failures appear to be independent of the target or technology employed. All classes of warheads have suffered clinical failures, including several recent failures by PBD-based ADCs, largely due to toxicity typically associated with the cytotoxic agent. Advances in ADC technology continue to offer promise to widen the therapeutic index. Similarly, a better understanding of the underlying biology and mechanisms of action of the cytotoxic agents may provide opportunity to widen the therapeutic index of ADCs. Herein we provide further evidence that tumor cells with underlying defects in DNA damage response (DDR) pathways, such as mutation or loss of *BRCA1/2*, may be hypersensitive to PBD-based ADCs.

Likewise, combinations with inhibitors of DDR pathways such as the PARPi olaparib demonstrated here can further enhance the antitumor activity. This supports testing expanded patient selection strategies for ADCs beyond just target expression and to think about rational combination strategies based on warhead mechanism of action as a way to further enhance the therapeutic index of ADCs.

In this study, 5T4-PBD was used as an exemplary ADC to further explore these hypotheses in preclinical models. 5T4 is a target of both active and failed ADCs and has been well characterized as an ADC target in preclinical models (36). Therefore, it served as a logical surrogate in these studies to deliver the PBD payload to tumor cells. The mechanism of action of the PBD is expected to be the critical factor when exploring biomarkers of activity and drug combination strategies. To this end, we did not observe any dependence on 5T4 expression levels provided that it was expressed at a sufficient level to deliver PBD inside the cell. This finding is consistent with the results previously reported by Sutherland and colleagues who demonstrated that CD33A-PBD retained potent cytotoxicity even in cells with low expression of CD33 (40). Cell models that do not express 5T4 do not show the same effects (Supplementary Fig. S6) and activity was observed well above control IgG-PBD so it is anticipated that target expression is still a critical variable to consider in patient selection.

The strengths of this study include the use of a panel of *BRCA*-deficient PDX models that allowed us to test the clinical potential

Zhong et al.

**Figure 5.**

Tolerability of 5T4-PBD in combination with olaparib in naïve nude mice. Single dose of 5T4-PBD (0.1 mg/kg) was administered on day 0. Olaparib (100 mg/kg) was given daily from day 0–15. Whole blood was collected via orbital bleeding on day 2, day 9, day 13, day 20, and day 27 for automated CBC determinations. Statistical significance was evaluated using Student *t* test. (*, *P* < 0.05 vs. untreated; **, *P* < 0.01 vs. untreated).

of this treatment protocol. Cell line xenograft models are generally not considered reliable predictors of clinical activity due to the clonal selection process on plastic. PDX, on the other hand, recapitulate the genetic diversity found in human tumors and properly mimic intratumoral heterogeneity. Confidence in pre-clinical outcomes can be greatly increased by using a panel of PDX models for each tumor type. In our case, we selected 23 breast or ovarian PDX models based on their *BRCA* gene-deficient status, and were blinded to target 5T4 expression. We demonstrated that

a single dose of PBD-based ADC at 0.3 mg/kg induced tumor regression with DCR of 74% in *BRCA*-deficient PDX models. Three fractionated doses of 0.1 mg/kg administered every 3 weeks resulted in similar DCR of 61%. Lower dose of ADC and increased dosing intervals may further minimize ADC-induced toxicity, as we have previously shown that fractionated dosing improved tolerability of PBD-based ADCs without impacting antitumor activity (41). Although our study is focused on breast and ovarian cancer, we expect that our results can be extended to other *BRCA*-

mutated cancers, such as prostate and pancreatic tumors, that are vulnerable to PBD-based ADCs.

Even though the PBD-based ADCs demonstrated impressive antitumor efficacy in the majority of *BRCA*-mutant tumors in our study, some *BRCA*-mutated tumors did not respond regardless of target expression level. It is possible that some tumors may require defects in more DNA repair proteins in addition to *BRCA* to demonstrate hypersensitivity to PBD treatment. In fact, our finding showing decreased expression of multiple DDR proteins in DLD1 *BRCA2*^{-/-} cells suggests that defects in other DDR proteins may contribute to the high sensitivity observed with PBD-based ADC in *BRCA*-deficient cells (Fig. 2E). Previously, McCabe and colleagues showed that the sensitivity of *BRCA*-deficient cells to PARP inhibition was due to a defect in DNA damage signaling proteins, such as RAD51, RAD54, DSS1, RPA1, NBS1, ATR, ATM, CHK1, CHK2, FANCD2, FANCA, or FANCC, rather than a deficiency in *BRCA1* or *BRCA2* per se (42). Similarly, loss of tumor suppressor INPP4B resulted in a DNA repair defect and increased sensitivity to PARP inhibitor due to concomitant loss of *BRCA1*, ATR, and ATM (43). Interestingly, many of the PDX models examined in our study also carry mutations including PTEN, p53, ATM, and ATR. Further characterization of other DDR proteins or oncogenic pathways and understanding how they are associated with response to PBD-based ADC is currently underway. It is our hope to identify other genes besides *BRCA1/2* that may contribute to the "BRCAness" of tumors, and to understand how other signaling pathways interplay with DDR pathway and whether this can be therapeutically exploited.

Following PBD-based ADC treatment, the *BRCA*-mutated cancer cells are unable to repair DSB and undergo cell death, or the cells rely on the base excision machinery to repair PBD-based damage via the enzyme PARP. PARPi have been shown to effectively kill *BRCA*-deficient tumors by preventing cells from repairing DNA. Therefore, we hypothesized that the antitumor effect of PBD-based ADC in *BRCA*-mutated tumors could be further enhanced with concomitant PARP inhibition. By combining PBD-based ADC with a PARPi, there would be an increased accumulation of DSB due to the inability of DNA repair pathways to repair the damage with high fidelity, therefore causing cell death. Approaches combining PARPi with other DNA-damaging agents have been explored. A number of preclinical studies in various cancer types, such as breast, ovarian, and prostate cancer, have shown that PARP inhibition can enhance the effects of some chemotherapies and ionizing radiation. In addition to agents that directly interact with DNA and cause DSB, agents that inhibit topoisomerase 1, such as irinotecan, have been shown to synergize with PARPi. Recently, Cardillo and colleagues demonstrated that combining the anti-Trop-2-SN-38 ADC (IMMU-132) with PARPi resulted in synergistic growth inhibition in triple-negative breast cancer tumors, regardless of *BRCA1/2* status (34). Here, we show that suboptimal dose of PBD-based ADC in combination with olaparib resulted in significantly enhanced antitumor effects compared with monotherapy in mice bearing *BRCA2*-deleted tumors. While *BRCA* wild-type tumors can still respond to PBD-based ADCs at significantly higher doses, these tumors do not respond to PARPi monotherapy. Consequently, we did not observe any synergy in this setting with the combination treatment, unlike in *BRCA*-mutated tumors. This contrasts with the observation by Cardillo and colleagues suggesting there may either be differences in how cells repair damage induced by

SN-38 compared with PBD or that other differences exist between DDR pathways used in the cell line models.

Because the therapeutic window is determined by efficacy and safety, the tolerability of PBD-based ADC in combination with olaparib was also evaluated in tumor-bearing and naïve mice. One noteworthy finding from our tolerability study was that 5T4-PBD plus olaparib combination therapy was well-tolerated in mice, with no effect on body weight change and little evidence of hematologic toxicity during and after the course of treatment. Together, the data demonstrate the potential for an increased therapeutic window by combining PBD-based ADC with a PARPi, as a result of significantly enhanced efficacy and improved tolerability in treating a subset of patients with *BRCA*-deficient cancers. The combination strategy may be particularly advantageous for indications in which PARPi has been approved.

In conclusion, here we demonstrate that both *BRCA1* and *BRCA2* mutation status are key factors in determining the sensitivity to PBD-based ADCs. Our results show a markedly increased sensitivity to PBD-based ADC in *BRCA*-deficient tumors. Moreover, we have demonstrated that PBD-based ADC in combination with PARPi has a widened therapeutic window with improved efficacy and better tolerability in treating *BRCA*-deficient tumors. These results suggest a novel strategy for treating patients with *BRCA*-mutated tumors.

Disclosure of Potential Conflicts of Interest

B.W. Higgs has ownership interest (including stock, patents, etc.) in AstraZeneca. A.J. Pierce is an associate director at AstraZeneca. R. Herbst has ownership interest (including stock, patents, etc.) in AstraZeneca. No potential conflicts of interest were disclosed by other authors.

Authors' Contributions

Conception and design: H. Zhong, C. Chen, J. Harper, A.J. Pierce, D.A. Tice
Development of methodology: H. Zhong, C. Chen, J. Zhang, R. Raja, J. Harper
Acquisition of data (provided animals, acquired and managed patients, provided facilities, etc.): H. Zhong, C. Chen, R. Tammali, S. Breen, C. Fazzenbaker, M. Kennedy, N. Holoweckyj, R. Raja
Analysis and interpretation of data (e.g., statistical analysis, biostatistics, computational analysis): H. Zhong, C. Chen, S. Breen, J. Zhang, C. Fazzenbaker, J. Conway, B.W. Higgs, J. Harper
Writing, review, and/or revision of the manuscript: H. Zhong, C. Chen, S. Breen, J. Conway, B.W. Higgs, J. Harper, A.J. Pierce, R. Herbst, D.A. Tice
Administrative, technical, or material support (i.e., reporting or organizing data, constructing databases): H. Zhong, C. Chen, J. Zhang, M. Kennedy, R. Raja
Study supervision: H. Zhong, C. Chen, D.A. Tice

Acknowledgments

The authors thank colleagues from Spirogen and Medimmune ADPE department for synthesizing PBD payload and completing ADC conjugations, Steven Durant from the olaparib team, and Gareth Davies for helpful discussion. We also thank Xentech, Champions, and South Texas Accelerated Research Therapeutics (START) for conducting *in vivo* experiments in patient-derived xenograft (PDX) models under service agreements. This work was supported by Medimmune.

The costs of publication of this article were defrayed in part by the payment of page charges. This article must therefore be hereby marked *advertisement* in accordance with 18 U.S.C. Section 1734 solely to indicate this fact.

Received March 26, 2018; revised July 31, 2018; accepted October 16, 2018; published first October 23, 2018.

References

1. Tolcher AW. Antibody drug conjugates: lessons from 20 years of clinical experience. *Ann Oncol* 2016;27:2168–72.
2. Gerber HP, Kung-Sutherland M, Stone I, Morris-Tilden C, Miyamoto J, McCormick R, et al. Potent antitumor activity of the anti-CD19 auristatin antibody drug conjugate hBU12-vcMMAE against rituximab-sensitive and -resistant lymphomas. *Blood* 2009;113:4352–61.
3. Lambert JM, Chari RV. Ado-trastuzumab Emtansine (T-DM1): an antibody–drug conjugate (ADC) for HER2-positive breast cancer. *J Med Chem* 2014;57:6949–64.
4. Bose DS, Thompson AS, Ching J, Hartley JA, Berardini MD, Jenkins TC, et al. Rational design of a highly efficient irreversible DNA interstrand cross-linking agent based on the pyrrolobenzodiazepine ring system. *J Am Chem Soc* 1992;114:4939–41.
5. Gregson SJ, Howard PW, Hartley JA, Brooks NA, Adams LJ, Jenkins TC, et al. Design, synthesis, and evaluation of a novel pyrrolobenzodiazepine DNA-interactive agent with highly efficient cross-linking ability and potent cytotoxicity. *J Med Chem* 2001;44:737–48.
6. Hartley JA, Spanswick VJ, Brooks N, Clingen PH, McHugh PJ, Hochhauser D, et al. SJG-136 (NSC 694501), a novel rationally designed DNA minor groove interstrand cross-linking agent with potent and broad spectrum antitumor activity: part 1: cellular pharmacology, *in vitro* and initial *in vivo* antitumor activity. *Cancer Res* 2004;64:6693–9.
7. Alley MC, Hollingshead MG, Pacula-Cox CM, Waud WR, Hartley JA, Howard PW, et al. SJG-136 (NSC 694501), a novel rationally designed DNA minor groove interstrand cross-linking agent with potent and broad spectrum antitumor activity: part 2: efficacy evaluations. *Cancer Res* 2004;64:6700–6.
8. Hartley JA, Hamaguchi A, Coffils M, Martin CRH, Suggitt M, Chen Z, et al. SG2285, a novel C2-Aryl-substituted pyrrolobenzodiazepine dimer pro-drug that cross-links DNA and exerts highly potent antitumor activity. *Cancer Res* 2010;70:6849–58.
9. Janjigian YY, Lee W, Kris MG. A phase I trial of SJG-136(NSC#694501) in advanced solid tumors. *Cancer Chemother Pharmacol* 2010;65:833–8.
10. Stein AS, Walter RB, Erba HP, Fathi AT, Advani AS, Lancet JE, et al. A phase 1 trial of SGN-CD33A as monotherapy in patients with CD33-positive acute myeloid leukemia (AML). *Blood* 2015;126:324.
11. Rudin CM, Pietanza MC, Bauerv TM, Spigel DR, Ready N, Morgensztern D, et al. Safety and efficacy of single-agent rovalpituzumab tesirine (SC16LD6.5), a delta-like protein 3 (DL3)-targeted antibody-drug conjugate (ADC) in recurrent or refractory small cell lung cancer (SCLC). *J Clin Oncol* 34:18s, 2016(suppl; abstr LBA8505).
12. Powell SN, Kachnic LA. Roles of BRCA1 and BRCA2 in homologous recombination, DNA replication fidelity and the cellular response to ionizing radiation. *Oncogene* 2003;22:5784–91.
13. Kobayashi H, Ohno S, Sasaki Y, Matsuura M. Hereditary breast and ovarian cancer susceptibility genes (review). *Oncol Rep* 2013;30:1019–29.
14. Russo A, Calo V, Bruno L, Rizzo S, Bazan V, Di Fede G. Hereditary ovarian cancer. *Crit Rev Oncol Hematol* 2009;69:28–44.
15. Hud T, Rago C, Gallmeier E, Brody JR, Gorospe M, Kern SE. A syngeneic variance library for functional annotation for human variant: application to BRCA2. *Cancer Res* 2008;68:5023–30.
16. Evers B, Drost R, Schut E, de Bruin M, van der Burg E, Derksen PW, et al. Selective inhibition of BRCA2-deficient mammary tumor cell growth by AZD2281 and cisplatin. *Clin Cancer Res* 2008;14:3914–25.
17. Ame JC, Spenlehauser C, de Murcia G. The PARP superfamily. *Bioessays* 2004;26:882–93.
18. Bryant HE, Schultz N, Thomas HD, Parker KM, Flower D, Lopez E, et al. Specific killing of BRCA2-deficient tumors with inhibitors of poly(ADP-ribose) polymerase. *Nature* 2005;434:913–7.
19. Farmer H, McCabe N, Lord CJ, Tutt AJ, Johnson DA, Richardson TB, et al. Targeting the DNA repair defect in BRCA mutant cells as a therapeutic strategy. *Nature* 2005;434:917–21.
20. Gelmon KA, Tischkowitz M, Mackay H, Swenerton K, Robidoux A, Tonkin K, et al. Olaparib in patients with recurrent high-grade serous or poorly differentiated ovarian carcinoma or triple-negative breast cancer: a phase 2, multicentre, open-label, non-randomised study. *Lancet Oncol* 2011;12:852–61.
21. Marulonis UA, Harter P, Gourley C, Friedlander M, Vergote I, Rustin G, et al. Olaparib maintenance therapy in patients with platinum-sensitive, relapsed serous ovarian cancer and a BRCA mutation: overall survival adjusted for postprogression poly(adenosine diphosphate ribose) polymerase inhibitor therapy. *Cancer* 2016;122:1844–52.
22. Kristeleit R, Shapiro GI, Burris HA, Oza AM, LoRusso PM, Patel MR, et al. A phase I-II study of the oral poly(ADP-ribose) polymerase inhibitor rucaparib in patients with germline BRCA1/2-mutated ovarian carcinoma or other solid tumors. *Clin Cancer Res* 2017;23:4095–106.
23. Solmlo G, Frankel P, Arun B, Ma CX, Garcia A, Cigler T, et al. Efficacy of the PARP inhibitor veliparib with carboplatin or as a single agent in patients with germline BRCA1- or BRCA2-associated metastatic breast cancer. *Clin Cancer Res* 2017;23:4066–76.
24. de Bono J, Ramanathan RK, Mina L, Chugh R, Glaspy J, Rafi S, et al. Phase I, dose-escalation, two-part trial of the PARP inhibitor talazoparib in patients with advanced germline BRCA1/2 mutations and selected sporadic cancers. *Cancer Discov* 2017;7:620–9.
25. Scott LJ. Niraparib: first global approval. *Drugs* 2017;77:1029–34.
26. Ledermann J, Harter P, Gourley C, Friedlander M, Vergote I, Rustin G, et al. Olaparib maintenance therapy in platinum-sensitive relapsed ovarian cancer. *N Engl J Med* 2012;366:1382–92.
27. Ledermann J, Harter P, Gourley C, Friedlander M, Vergote I, Rustin G, et al. Olaparib maintenance therapy in patients with platinum-sensitive relapsed serous ovarian cancer: a preplanned retrospective analysis of outcomes by BRCA status in a randomised phase 2 trial. *Lancet Oncol* 2014;15:852–61.
28. Kummur S, Oza AM, Fleming GF, Sullivan DM, Gandara DR, Naughton MJ, et al. Randomized trial of oral cyclophosphamide and veliparib in high-grade serous ovarian, primary peritoneal, or fallopian tube cancers, or BRCA-mutant ovarian cancer. *Clin Cancer Res* 2015;21:1574–82.
29. Albert JM, Cao C, Kim KW, Willey CD, Geng L, Xiao D, et al. Inhibition of poly(ADP-ribose) polymerase enhances cell death and improves tumor growth delay in irradiated lung cancer models. *Clin Cancer Res* 2007;13:3033–42.
30. Chatterjee P, Choudhary GS, Sharma A, Singh K, Heston WD, Ciezki J, et al. PARP inhibition sensitizes to low dose-rate radiation TMPRSS2-ERG fusion gene-expressing and PTEN-deficient prostate cancer cells. *PLoS One* 2013;8:e60408.
31. Barreto-Andrade JC, Efimova E, Mauceri HJ, Beckett MA, Sutton HG, Darga TE, et al. Response of human prostate cancer cells and tumors to combining PARP inhibition with ionizing radiation. *Mol Cancer Ther* 2011;10:1185–93.
32. Gani C, Coacklet C, Kumareswaran R, Schutze C, Krause M, Zafarana G, et al. *In vivo* studies of the PARP inhibitor, AZD-2281, in combination with fractionated radiotherapy: an exploration of the therapeutic ratio. *Radiother Oncol* 2015;116:486–94.
33. Rottenberga S, Jaspersa JE, Kersbergena A, van der Burg E, Nygren AO, Zander SA, et al. High sensitivity of BRCA1-deficient mammary tumors to the PARP inhibitor AZD2281 alone and in combination with platinum drugs. *Proc Natl Acad Sci U S A* 2008;105:17079–84.
34. Cardillo TM, Sharkey RM, Rossi DL, Arrojo R, Mostafa AA, Goldenberg DM. Synthetic lethality exploitation by an anti-Trop-2-SN-38 antibody-drug conjugate, IMMU-132, plus PARP-inhibitors in BRCA1/2-wild-type triple-negative breast cancer. *Clin Cancer Res* 2017;23:3405–15.
35. Langmead B, Salzberg SL. Fast gapped-read alignment with Bowtie 2. *Nat Methods* 2012;9:357–9.
36. Harper J, Lloyd C, Dimasi N, Toader D, Marwood R, Lewis L, et al. Preclinical evaluation of MEDI0641, a pyrrolobenzodiazepine-conjugated antibody-drug conjugate targeting 5T4. *Mol Cancer Ther* 2017;16:1576–87.
37. Konish H, Mohseni M, Tamaki A, Garay JP, Croessmann S, Karnan S, et al. Mutation of a single allele of the cancer susceptibility gene BRCA1 leads to

- genomic instability in human breast epithelial cells. *Proc Natl Acad Sci U S A* 2011;108:17773–8.
38. Mah LJ, El-Osta A, Karagiannis TC. gammaH2AX: a sensitive molecular marker of DNA damage and repair. *Leukemia* 2010;24:679–86.
 39. Byrski T, Dent R, Blecharz P, Foszczynska-Kloda M, Gronwald J, Huzarski T, et al. Results of a phase II open-label, non-randomized trial of cisplatin chemotherapy in patients with BRCA1-positive metastatic breast cancer. *Breast Cancer Res* 2012;14:R110.
 40. Sutherland MS, Walter RB, Jeffrey SC, Burke PJ, Yu C, Kostner H, et al. SGN-CD33A: a novel CD33-targeting antibody-drug conjugate using a pyrrolobenzodiazepine dimer is active in models of drug-resistant AML. *Blood* 2013;122:1455–63.
 41. Hinrichs MJ, Ryan PM, Zheng B, Afif-Rider S, Yu X, Gonsior M, et al. Fractionated dosing improves preclinical therapeutic index of pyrrolobenzodiazepine-containing antibody drug conjugates. *Clin Cancer Res* 2017;23:5858–68.
 42. McCabe N, Turner NC, Lord CJ, Kluzek K, Bialkowska A, Swift S, et al. Deficiency in the repair of DNA damage by homologous recombination and sensitivity to poly(ADP-ribose) polymerase inhibition. *Cancer Res* 2006;66:8109–15.
 43. Ip LR, Poulogiannis G, Viciano FC, Sasaki J, Kofuji S, Spanswick VJ, et al. Loss of INPP4B causes a DNA repair defect through loss of BRCA1, ATM and ATR and can be targeted with PARP inhibitor treatment. *Oncotarget* 2015;6:10548–62.

Molecular Cancer Therapeutics

Improved Therapeutic Window in *BRCA*-mutant Tumors with Antibody-linked Pyrrolobenzodiazepine Dimers with and without PARP Inhibition

Haihong Zhong, Cui Chen, Ravinder Tammali, et al.

Mol Cancer Ther 2019;18:89-99. Published OnlineFirst October 23, 2018.

Updated version Access the most recent version of this article at:
doi:[10.1158/1535-7163.MCT-18-0314](https://doi.org/10.1158/1535-7163.MCT-18-0314)

Supplementary Material Access the most recent supplemental material at:
<http://mct.aacrjournals.org/content/suppl/2018/10/23/1535-7163.MCT-18-0314.DC1>

Cited articles This article cites 42 articles, 18 of which you can access for free at:
<http://mct.aacrjournals.org/content/18/1/89.full#ref-list-1>

Citing articles This article has been cited by 1 HighWire-hosted articles. Access the articles at:
<http://mct.aacrjournals.org/content/18/1/89.full#related-urls>

E-mail alerts [Sign up to receive free email-alerts](#) related to this article or journal.

Reprints and Subscriptions To order reprints of this article or to subscribe to the journal, contact the AACR Publications Department at pubs@aacr.org.

Permissions To request permission to re-use all or part of this article, use this link
<http://mct.aacrjournals.org/content/18/1/89>.
Click on "Request Permissions" which will take you to the Copyright Clearance Center's (CCC) Rightslink site.